Research Article

A First Vascularized Skin Equivalent as an Alternative to Animal Experimentation

Florian Groeber [1], Lisa Engelhardt [2], Julia Lange [3], Szymon Kurdyn [2], Freia F. Schmid [1], Christoph Rücker [2], Stephan Mielke [3], Heike Walles [1,2] and Jan Hansmann [1,2]

[1]Translational Center Würzburg, Fraunhofer Institute for Interfacial Engineering and Biotechnology (IGB) Würzburg, Germany; [2]Chair of Tissue Engineering and Regenerative Medicine, University Hospital Würzburg, Würzburg, Germany; [3]Department of Internal Medicine II, University Hospital Würzburg, Würzburg, Germany

Summary

Tissue-engineered skin equivalents mimic key aspects of the human skin and can thus be employed as wound coverage for large skin defects or as *in vitro* test systems as an alternative to animal models. However, current skin equivalents lack a functional vasculature, limiting clinical and research applications. This study demonstrates the generation of a vascularized skin equivalent with a perfused vascular network by combining a biological vascularized scaffold (BioVaSc) based on a decellularized segment of porcine jejunum and a tailored bioreactor system. The BioVaSc was seeded with human fibroblasts, keratinocytes, and human microvascular endothelial cells. After 14 days at the air-liquid interface, hematoxylin & eosin and immunohistological staining revealed a specific histological architecture representative of the human dermis and epidermis, including a papillary-like architecture at the dermal-epidermal-junction. The formation of the skin barrier was measured non-destructively using impedance spectroscopy. Additionally, endothelial cells lined the walls of the formed vessels that could be perfused with a physiological volume flow. Due to the presence of a complex *in vivo*-like vasculature, the here shown skin equivalent has the potential to be used for skin grafting and represents a sophisticated *in vitro* model for dermatological research.

Keywords: skin equivalents, alternative to animal testing, vascularization, tissue engineering

1 Introduction

Tissue-engineered, three-dimensional skin equivalents are capable of mimicking key anatomical, metabolic, cellular and functional aspects of native human skin. Thus, they can be employed as wound coverage for large skin defects or as *in vitro* test systems instead of animal models in basic research (Groeber et al., 2011). Generally, two types of tissue-engineered skin models are available, being representatives of either the epidermis alone (reconstructed human epidermis) or the dermal and epidermal layer (full-thickness skin equivalents) (De Wever et al., 2013). In spite of recent progress, the use of current skin equivalents for medical purposes and as test systems remains limited owing to the lack of a functional vasculature.

In skin transplantation, an existing vasculature supports a rapid anastomosis of donor skin to the host's vasculature (inosculation), whereas for tissue-engineered skin implants, new vessels must be formed by angiogenesis, which delays graft integration (Young et al., 1996). Consequently, bio-engineered skin implants are more likely to be rejected. In addition, the cutaneous vasculature is crucial for several physiological and pathophysiological processes including the development of skin diseases, wound healing, metastasizing of malignant melanoma, tumor-angiogenesis, auto- and alloimmune-phenomena, and the transdermal penetration of substances. Taken together, non-vascularized skin models are of limited value with regard to their ability to reflect the physiological conditions of a full organ. In the absence of a model that represents the physiological conditions of a full organ, there remains a scientific and medical need for animal models.

To overcome these limitations, endothelial cells can be seeded into the dermal part of full-thickness skin equivalents, which results in the alignment of endothelial cells to vessel-like struc-

Abbreviations

BioVaSc, biological vascularized scaffold; hDMEC, human dermal microvascular endothelial cells; hDF, human dermal fibroblasts; hEK, human epidermal keratinocytes; MTT, 3-(4,5-dimethylthiazol-2-yl)-2,5-diphenyltetrazoliumbromide

Received April 4, 2016;
Accepted May 3, 2016;
Epub May 15, 2016;
http://dx.doi.org/10.14573/altex.1604041

tures (Lei et al., 2011; Montano et al., 2010; Schechner et al., 2003; Shepherd et al., 2006; Supp et al., 2002; Tremblay et al., 2005). However, in these models no functional perfusable vasculature is formed *in vitro*. Thus, those pre-vascularized skin equivalents cannot be directly anastomosed to a patient's blood flow, and the vasculature is not experimentally accessible.

To generate perfusable vascularized tissues, a biological vascularized scaffold (BioVaSc) can be used. This scaffold serves as a platform technology for the generation of different vascularized tissue equivalents such as liver (Linke et al., 2007) or trachea (Mertsching et al., 2009). The BioVaSc is based on a decellularized segment of a porcine jejunum that is supplied by a single artery-vein-pair (Mertsching et al., 2008; Walles et al., 2004). The scaffold mainly consists of collagen type III and type I and also comprises structures of the former native vascular network. By reseeding these structures with human endothelial cells, a closed perfusable vascular network can be generated. However, a pivotal aspect of the BioVaSc technology is the bioreactor required for tissue maturation. The bioreactor system generates a physiological medium flow into the vasculature of the BioVaSc with a pulsatile pressure profile between 80 and 120 mmHg. Moreover, the bioreactor system supports culturing of the BioVaSc under submerged conditions as well as at the air-liquid-interface, which is a crucial requirement to trigger the formation of a functional skin barrier (Groeber et al., 2013).

The hypothesis of this study was that using the BioVaSc in combination with the custom developed bioreactor system allows generation of a vascularized skin equivalent with a perfused vascular network *in vitro*. For this, the embedded vascular structures in the BioVaSc are reseeded with human dermal microvascular endothelial cells (hDMEC) before skin tissue is constructed by seeding the surface with human dermal fibroblasts (hDF) and human epidermal keratinocytes (hEK). Here, we describe for the first time the development of a functional and fully vascularized human skin model employing the BioVaSc strategy. This model mimics physiological conditions of a full human skin organ and may thus serve as an optimized substitute for animal models in medical research.

2 Material and methods

Ethical clearance statement

Primary cells were isolated from foreskin biopsies from juvenile donors aged between 1 and 3 years. All donors' legal representative(s) provided full informed consent in writing. The study was approved by the local ethical board of the University of Würzburg (vote 182/10) and the *Landesärztekammer Baden-Württemberg* (IGBZSF-2012-078). For scaffold preparation, porcine jejunal segments were obtained from German Landrace pigs (weighing 15 to 25 kg). The animals received humane care in compliance with the Directive 2010/63/EU of the European Parliament and of the Council of 22 September 2010 on the protection of animals used for scientific purposes and the German Animal Welfare Act (last amended by Art. 3 G v. 28.7.2014 I 1308) after approval from our institutional animal protection board.

Cell isolation and culture

Human epidermal keratinocytes, human dermal fibroblasts and human microvascular endothelial cells were isolated from foreskin biopsies according to previously published protocols (Groeber et al., 2013; Pudlas et al., 2011; Rossi et al., 2015). After isolation, keratinocytes were cultured in Keratinocyte Growth Medium (KGM) supplemented with KGM supplement mix (both from PromoCell, Heidelberg, Germany) and 1% penicillin/streptomycin (Life Technologies GmbH, Darmstadt, Germany). Fibroblasts were cultured in Dulbecco's modified Eagle medium (DMEM, Life Technologies GmbH) with 10% fetal bovine serum (Sigma-Aldrich Chemie GmbH, Schnelldorf, Germany) supplemented with 1% penicillin/streptomycin. Microvascular endothelial cells were cultured in VascuLife Basal medium supplemented with VascuLife EnGS LifeFactors (both from Life Technologies GmbH) and 1% penicillin/streptomycin. For all cell types, medium was changed every two to three days. Cells were used for experiments once 80 to 90% confluency was reached. Keratinocytes were used from first to second passage and both fibroblasts and microvascular endothelial cells from second to fifth passage.

Generation of a vascularized skin equivalent

The BioVaSc matrix was prepared using a previously described protocol (Mertsching et al., 2009; Scheller et al., 2013). Briefly, an approximately 15 cm long segment of a porcine jejunum that was supplied by a single artery-vein-pair was explanted carefully without harming the outer vascular system. Tissue diameter was dependent on the respective animal and varied between 2 and 4 cm. The native tissue was decellularized by perfusing the vasculature with sodium-desoxycholate under constant pressure conditions at 100 mmHg. After sterilization by gamma irradiation, the matrix was stored at 4°C. To generate the vascularized skin equivalent, the BioVaSc was cut longitudinally on the antimesenteric side and fixed in a polycarbonate frame. After equilibration in VascuLife EnGS Medium Complete Kit, (Life Technologies GmbH) for 24 h at 37°C and 5% CO_2 in a humidified incubator, vessels were reseeded with $1*10^7$ hDMEC in 1000 µl. For this, 700 µl of the cell suspension was injected into the arterial inlet and 300 µl into the venous inlet via a sterile syringe. Directly after, the surface of the model was inoculated with $1.86*10^5$ hDF. The BioVaSc was placed in a previously published bioreactor system, in which the vasculature was connected to a fluidic circuit (Groeber et al., 2013). Initially, perfusion was started with a pressure of 10 mmHg, increased stepwise to 80 mmHg, and then changed to a physiological pulsatile pressure profile with a systolic pressure of 120 mmHg and diastolic pressure of 80 mmHg. Additionally, a second and third fluidic circuit delivered medium to the surface and lower side, respectively. Culturing under these submerged conditions was continued until day 6. In the next step, the cell culture medium was replaced by hEK medium supplemented with 5% FBS and $1.86*10^6$ hEK were seeded on the surface of the model. On day 9 and 12 the FBS concentration was lowered to 2% and 0%, respectively. Cell culture medium was replaced by KGM medium supplemented with KGM supplement mix (both from PromoCell), and 1.5 mM $CaCl_2$ (Sigma-Aldrich Chemie) and

1% penicillin/streptomycin (Life Technologies GmbH) medium and the bioreactor was switched to air-liquid interface conditions on day 13 as described in our previous publication (Groeber et al., 2013). Briefly, a two-way selector valve was changed so that instead of cell culture medium, sterile air was directed over the surface of the model. Culture was continued until day 27, whereby cell culture medium was exchanged on day 20. The culture in the bioreactor system was performed in a tailor-designed incubation system with programmable pumps under 37°C and 5% CO_2.

Histological analysis

Samples were fixed in Histofix® (Carl Roth GmbH; Karlsruhe, Germany) and embedded in paraffin. Cross sections of 3 µm thickness were stained with hematoxylin & eosin (H&E) and covered in Isomount® (Labonord; Templemars, France) and bright-field images were obtained for general analysis of the morphological architecture. ImageJ software (National Institutes of Health) was used to measure histological features. For immunohistofluorescence staining, cross sections were hydrated and subjected to antigen retrieval in tris-ethylenediaminetetraacetic acid buffer (cytokeratin 14, cytokeratin 10, filaggrin, collagen type IV, CD-31, von Willebrand Factor) or citrate buffer (vimentin) for 20 minutes at 100°C. After blocking unspecific binding with goat (cytokeratin 14, cytokeratin 10, filaggrin, collagen type IV, CD-31, and von Willebrand Factor) or donkey serum (vimentin), 500 µl of primary antibody solution (cytokeratin 14, 1:500 (Sigma-Aldrich Chemie GmbH); cytokeratin 10, 1:500 (Dako; Glostrup, Denmark); filaggrin, 1:50 (Biomol GmbH; Hamburg, Germany); collagen type IV, 1:50 (abcam plc; Cambridge, United Kingdom); CD-31, 1:100 (Dako); von Willebrand Factor, 1:100 (Dako); vimentin, 1:1000 (abcam plc)) was applied and incubated for 12 h at 4°C. The primary antibody solution was removed and the secondary antibodies coupled with Alexa Fluor® 594 (cytokeratin 14, IgG1 anti rabbit 1:250 (Sigma-Aldrich Chemie GmbH); cytokeratin 10, filaggrin, collagen type IV, CD-31, and von Willebrand Factor IgG1 anti mouse 1:250 (Sigma-Aldrich Chemie GmbH)) or Alexa Fluor® 488 (vimentin, IgG1 anti rabbit 1:400 (Sigma-Aldrich Chemie GmbH)). After 1 h staining at room temperature, the slides were washed and all cell nuclei were counter-stained with 4',6-diamidino-2-phenylindole (DAPI (SouthernBiotech; Birmingham, United States)) and covered with ProLong® Gold Anti Fade.

Barrier assessment

The barrier of the vascularized skin equivalent was characterized non-destructively during tissue maturation by impedance spectroscopy (Groeber et al., 2015). Two electrodes – a working electrode in the lid of the bioreactor and a counter electrode underneath the tissue – allowed introducing a sinusoidal current *I(f)*. To record the impedance spectra of *Z(f)* from biological samples, the potential difference *U(f)* between the two electrodes was measured employing an impedance spectrometer LCR HiTESTER 3522-50 (HIOKI E.E. Corporation; Ueda, J). A tailored user interface, programmed in LabVIEW (National Instruments; Austin, USA), calculated the impedance *Z(f)* according to $Z(f)=U(f)/I(f)$. Hereby, *Z(f)*, *U(f)*, and *I(f)* are complex numbers. An electrical equivalent circuit facilitated extracting biologically relevant parameters from the spectra via a least

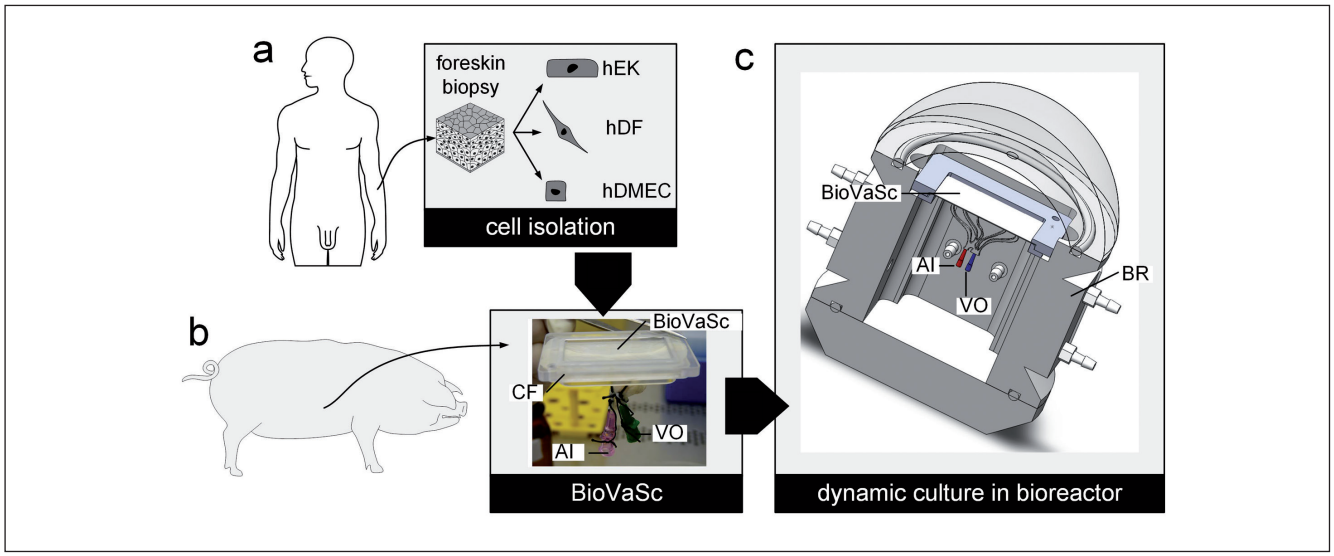

Fig. 1: Experimental procedure to generate the vascularized skin equivalent

a) In a first step, human epidermal keratinocytes (hEK), human dermal fibroblasts (hDF), and human dermal microvascular endothelial cells (hDMEC) are isolated from juvenile foreskin biopsies. b) Subsequently, the cells are seeded on a biological vascularized scaffold (BioVaSc) based on a decellularized segment of porcine jejunum. The acellular vascular structures of the BioVaSc are inoculated with hDMEC through the arterial inflow (AI) and venous outflow (VO). Additionally, hDF and hEK are seeded onto the surface of the BioVaSc. c) To allow the culture of the scaffold at air-liquid-interface, the BioVaSc is fixed in a frame (CF) and placed in a bioreactor (BR) system. In the BR the vascular system of the BioVaSc is perfused with a physiological pressure profile with a systolic pressure of 120 mmHg and diastolic pressure of 80 mmHg.

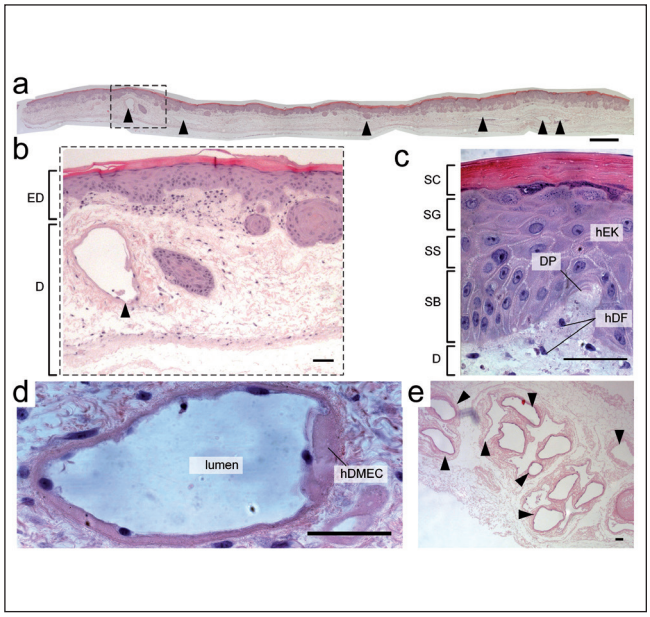

Fig. 2: Hematoxylin & eosin stained cross-section of the vascularized skin equivalent (vSE)
a) Overview of the vSE. b) Magnification of the area indicated in a. The vSE is composed of an epidermal (ED) and a dermal (D) part shaped by the biological vascularized scaffold (BioVaSc). c) Detailed view of the epidermal layer in which the human epidermal keratinocytes (hEK) build up the layered architecture with a clearly visible stratum basale (SB), stratum spinosum (SS), stratum granulosum (SG), and stratum corneum (SC). Underneath the epidermis is a dermal part with human dermal fibroblasts (hDF). d) Detailed image of a vascular structure that has been reseeded with human dermal microvascular endothelial cells (hDMEC). e) Image of the vasculature in efferent vessels. Black arrowheads indicate vascular structures in all images. Scale bars indicate 500 µm in a) and 50 µm in b)-e).

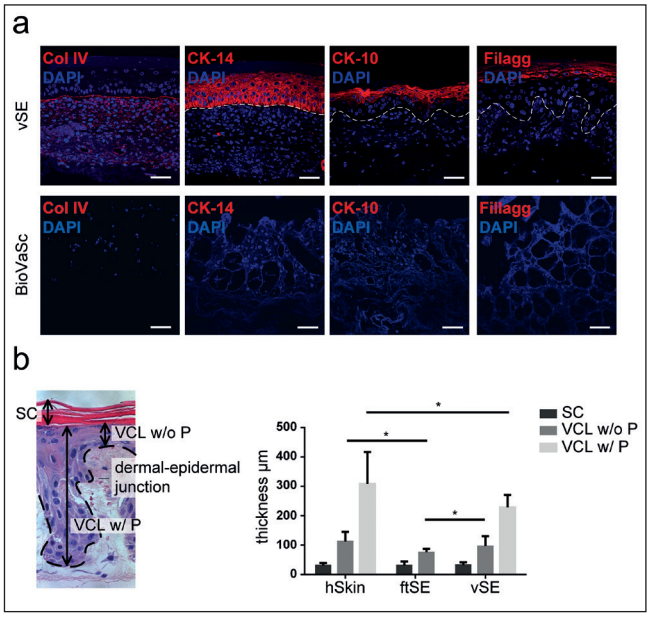

Fig. 3: Characterization of the epidermal layer
a) Analysis of epidermal markers in the vascularized skin equivalent (vSE) and the unseeded biological vascularized scaffold (BioVaSc) via immunohistological staining. Positive binding of primary antibodies against collagen type IV (Col IV), cytokeratin-14 (CK-14), cytokeratin-10 (CK-10), and filaggrin (filagg.) is visualized in red. Broken lines indicate the dermal-epidermal junction. Scale bars indicate 50 µm. b) Mean thickness and standard deviation of the stratum corneum and the viable cell layers in the human skin (hSkin), full-thickness skin equivalents (ftSE) and the vascularized skin equivalent (vSE). As the topography of the human skin and the vascularized skin equivalent is not flat, the thickness of the viable cell layers was measured either from the lowest point of the dermal papillae (VCL w/ P) or from the top of the dermal papillae (VCL w/o P). Statistically significant differences are indicated by stars (N = 22; $p \leq 0.05$).

square minimization algorithm (Matlab, Mathworks, Natick, USA). The tissue was described by an ohmic resistor and a capacitor in parallel connection.

Characterization of vasculature
Vessel network was visualized by staining viable cells with a 1 mg/ml solution of 3-(4,5-dimethylthiazol-2-yl)-2,5-diphenyltetrazoliumbromide (MTT) (Sigma-Aldrich Chemie GmbH) in VascuLife EnGS Medium Complete Kit (Life Technologies GmbH) for 3 h in a humidified atmosphere with 37°C and 5% CO_2. To measure the arterial inflow, the artery was connected to a peristaltic pump and the arterial pressure was set to 100 mmHg. The volume flow was calculated from the rotational speed of the peristaltic pump,.

Statistical analysis
Quantitative data was analyzed for statistically significant differences with GraphPad Prism® 6 using a one-way ANOVA employing Tukey's multiple comparisons test.

3 Results

3.1 Culture in the bioreactor facilitates the formation of a stratified epidermal and a vascularized dermal layer

To form the vascularized skin equivalent, hDMEC were seeded into the vascular system of the BioVaSc and the surface of the matrix was inoculated with hDF and hEK. Following culture at the air-liquid-interface in a specific-designed bioreactor system (Fig. 1), a well-stratified epidermis was formed on the BioVaSc. The epidermis covered the complete surface of 8 cm^2 (Fig. 2a). A higher magnification revealed that hDF were distributed homogenously in the BioVaSc forming the dermal layer (Fig. 2b). In addition, hEK differentiated into an epidermis with clearly distinguishable structural layers. The dermal-epidermal junction mimicked the structure of dermal papillae due to the topography of the biological scaffold (Fig. 2c). Tubular structures lined with hDMEC were found within the dermal component (Fig. 2c,d). Vessel density increased with proximity to the afferent vasculature (Fig. 2e).

3.2 Human keratinocytes form a correctly differentiated epidermis with an *in vivo*-like dermal-epidermal junction

Immunohistological staining against collagen type IV demonstrated the presence of basement membrane proteins at the dermal-epidermal junction. No collagen type IV was detected in the cell-free scaffold. Localization of cytokeratin-14 in the basal layer and presence of cytokeratin-10 in the supra-basal layers verified an anatomically correct differentiation of the epidermis. Moreover, positive filaggrin staining indicated the formation of a cornified layer (Fig. 3a).

The thickness of the stratum corneum and the viable cell layers was measured to compare the bioengineered epidermal layer with native human skin and standard full-thickness skin equivalents (Fig. 3b). To ensure comparability between the bioengineered skin equivalents, the models were analyzed after the same time in culture and histologically processed using the same buffer solutions and devices. Due to the presence of dermal invaginations, the distances from the stratum corneum to the tip of the dermal papillae and to the bottom of the invagination between the papillae, respectively, were determined separately for human skin and the vascularized skin equivalent, which is highlighted in Figure 3b. For the thickness of the stratum corneum, no significant difference was measured between the three experimental groups. The thickness of the viable cell layers of full thickness skin equivalents was statistically lower compared to both other groups. Although no significant difference could be found between human skin and the vascularized skin equivalent for the distance from the papillae tip to the stratum corneum, the height of the invagination between the papillae was significantly higher in human skin.

3.3 Vessel structures are populated with human endothelial cells and exhibit a higher diameter than vessels in human skin

To generate a functional endothelial network, hDMEC were seeded into the preserved structures of the former blood vessels of the jejunum. The hDMEC were able to colonize the tubular structures and formed an interconnected and branched network (Fig. 4a).

After 28 days of culture in the tailored bioreactor system, the formed re-endothelialized tubular structures were compared to the blood vessels of human skin by measuring the vessel diameters in the vascularized skin equivalent and the upper and lower plexus of human skin (Fig. 4b). The mean vessel diameter of the lower plexus (35 ± 22 µm) was significantly lower than in the upper plexus of human skin (101 ± 68 µm). Seeded vessels in the vascularized skin equivalent exhibited a broad diameter range with a significantly higher mean value (180 ± 105 µm) than both vessel plexuses. The vascular structures were embedded in a dermal layer. Immunohistological staining revealed homogenously distributed vimentin positive cells demonstrating the presence of hDF. Moreover, cells exhibiting endothelial cell markers CD31 and vWF were only found in the vascular structures. In contrast, the cell-free BioVaSc showed no staining for the analyzed markers (Fig. 4c).

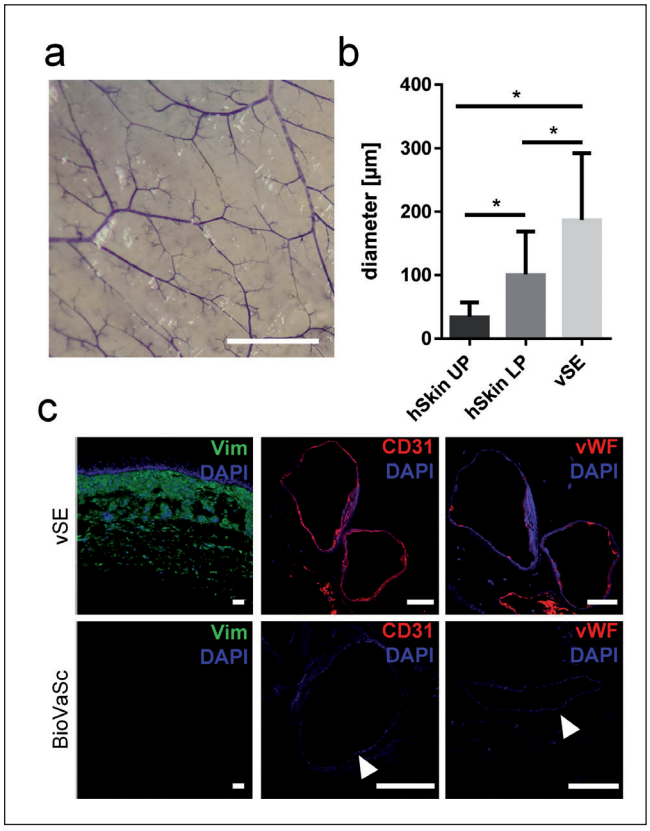

Fig. 4: Characterization of the dermal layer
a) Re-endothelialized vascular network of the biological vascularized scaffold (BioVaSc) stained with 3-(4,5-dimethylthiazol-2-yl)-2,5-diphenyltetrazoliumbromid (MTT). b) Mean values and standard deviation of vessel diameter in the upper (hSkin UP) and lower plexus (hSkin LP) of human skin and the vasculature within the dermis of the vascularized skin equivalent (vSE). Statistically significant differences are indicated by stars (N = 24; $p = 0.05$). c) Analysis of endothelial and fibroblast markers in the vSE and the unseeded BioVaSc via immunohistological staining. Positive binding of primary antibodies against CD31 (PECAM-1) and von Willebrand Factor (vWF) is depicted in red. White arrowheads point to the vascular structures. The fibroblasts show positive binding of primary antibodies against vimentin depicted in green. Scale bars indicate 500 µm in a), 50 µm in b) and c).

3.4 Non-destructive monitoring confirms the epidermal barrier and vessel perfusion

A vital aspect of skin equivalents is the formation of a strong epidermal barrier. To assess this criterion in a non-destructive manner, impedance spectra were measured and used to derive electrical characteristics of the skin model (Fig. 5a). During culture, the surface-normalized ohmic resistance increased by 192 Ω*cm^2, whereas the capacitance dropped by 12.3 µF/cm^2 (Fig. 5b).

To demonstrate vessel perfusion, arterial inflow was measured for the native tissue, for the cell-free BioVaSc, and for the re-endothelialized BioVaSc (Fig. 5c). Prior to decellulari-

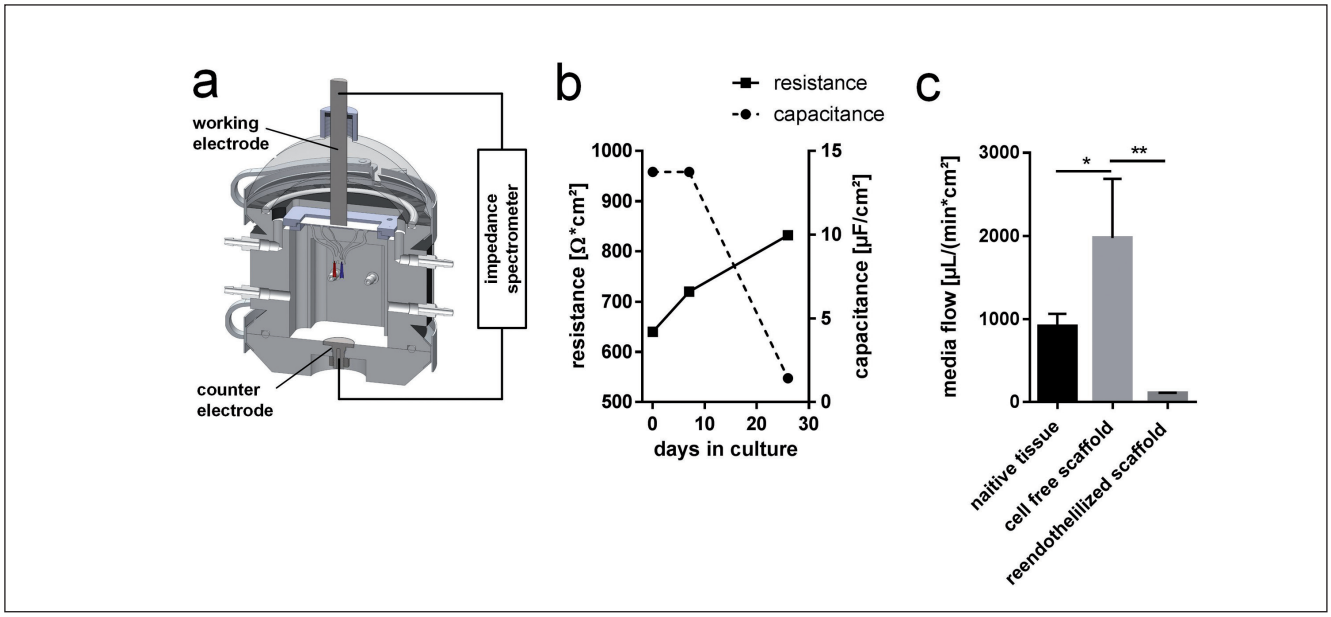

Fig. 5: Functional characterization of the vascularized skin equivalent

a) Impedance spectroscopy was employed to assess epidermal barrier formation non-destructively. A working and a counter electrode were introduced into the bioreactor and connected to an impedance spectrometer. b) Electrical characteristics were derived from the impedance spectra (exemplarily shown for one bioreactor). During culture, the surface-normalized ohmic resistance increased up to 832 Ω*cm² and the normalized capacitance decreased to 1.43 µF/cm². c) Perfusability was demonstrated by measuring the arterial inflow at 100 mmHg. Compared to the native tissue, the decellularization process led to an increased volume flow, whereas the re-endothelialization of the scaffold decreased the arterial inflow. Statistically significant differences are indicated by stars (N = 8; $p \leq 0.05$).

zation, the jejunal segment consumed a mean volume flow of 912.5 µl/(min*cm²) at 100 mmHg. Following removal of the porcine cells, arterial inflow was increased significantly to 1975 µl/(min*cm²). Reseeding of the vasculature with hDMEC reduced the cell culture medium flow into the artery to 109.2 µl/(min*cm²). Even though the measured inflow of the re-endothelialized BioVaSc was below that of the native tissue, the difference was not statistically significant.

4 Discussion

To overcome limitations of classical, non-vascularized skin models, we developed a fully vascularized human skin model employing the BioVaSc strategy. This model facilitates physiological vascular functions. The cutaneous vasculature is a complex network making it challenging to integrate vascular structures in an *in vitro* skin equivalent (Novosel et al., 2011). Despite technical advancements with methods such as bioprinting, the manufacturing of a network comparable to the *in vivo* situation is yet to be achieved. Hence, we employed a decellularized xenogenic matrix with conserved and perfusable vascular structures. In combination with a bioreactor system the scaffold facilitated the generation of a human vascularized skin equivalent. Although this approach involves the use of animal derived material as supporting scaffold, it should be noted that up to four jejunal segments can be explanted from one pig and that the number of used animals is reduced to a minimum since other tissues are used for further research purposes. The developed model was composed of an epidermal and a dermal layer. Vessel structures were present within the dermal part. As the skin equivalent is based on a jejunal matrix, the general architecture of the microcirculation is expected to reflect the anatomy of the porcine gut (Yao et al., 2012). This is reflected in the histological analysis that demonstrated a significantly higher vessel diameter in the vascularized skin equivalent compared to human skin. However, the generated vascular architecture where a branched capillary network is supplied by a larger artery-vein-pair is also comparable to the architecture of skin (Braverman, 2000). In the vascularized skin equivalent, a capillary system connected a central artery and a corresponding vein. A single layer of hDMEC lined the vessel walls and formed a clear vessel lumen. Although the histology of the model indicates an endothelial cell barrier, a vital aspect of vascular anatomy, further cellular components such as pericytes or muscle cells are missing.

The presence of tubular structures is a vital perquisite for the perfusion of the skin equivalent. Compared to the explanted intestinal tissue, the reseeded BioVaSc exhibited a lower arterial inflow, indicating some clogged vessels. Nevertheless, the measured inflow at 100 mmHg resulted in a perfusate of 100 µl/(min cm²). This correlates with the physiological perfusion of the skin capillary blood flow (Johnson et al., 1986) and facilitates a bidirectional mass transport into the surrounding

tissue across the endothelial barrier. As expected for skin tissue, vessels were only located in the dermal part. Here, hDF were homogenously distributed, allowing a close interaction between endothelial and stromal cells. At the dermal-epidermal junction, collagen type IV, a prominent basal membrane protein, could be detected. As no collagen type IV was detected in the cell-free scaffold, the presence of collagen type IV in the dermal-epidermal junction suggests *de novo* synthesis by the hEK, paralleling basement membrane formation in wound healing (Stark et al., 2004) and embryogenesis (Poschl et al., 2004). Moreover, the dermal-epidermal junction was aligned to the crypts of the former intestinal tissue that results in topography comparable to the dermal papillae of human skin. Due to the increased surface area, a higher mechanical resilience of the dermal-epidermal junction can be assumed compared to standard full-thickness skin equivalents with an even interface between dermis and epidermis. Moreover, the BioVaSc facilitated the attachment of hEK to the folded topography, resulting in a differentiated multilayer epidermis. Physiological differentiation was confirmed by immunohistological staining, showing a physiological location of cytokeratin-14 in the basal layer and cytokeratin-10 in the suprabasal layers (Fuchs, 2009). The differentiation also led to an even, stratified layer that was positive for filaggrin, which is essential for the corneous layer (Mildner et al., 2010). The integrity of the formed barrier could be demonstrated by measuring the electrical resistance during culture. The electrical barrier reached 192 Ω*cm^2, which is comparable to other *in vitro* models but below the value of human skin (Knott et al., 2008). The capacitance was investigated as a second electrical parameter. In a previous study, the reduction in capacitance, which was also shown in this study, was found to be predictive for an increase of tissue thickness (Groeber et al., 2015). In contrast to standard trans-epithelial electrical resistance values, the system used here shows a higher sensitivity, since the values are not biased by the electrical setup and electrode orientation. Furthermore, trans-epithelial electrical resistance measurements are limited to the ohmic resistance and extraction of further electrical parameters such as the capacitance is not possible.

The vascularized skin equivalent closely resembles the histological architecture of human skin and facilitates the cross-talk among vasculature, epidermal and dermal part. Also, the matrix provides stable vessel lumen, allowing the perfusion of the complex vascular network formed. To date, perfusion of vessel-like structures in pre-vascularized models has only been achieved upon grafting to an animal model (Gibot et al., 2010; Schechner et al., 2003; Tremblay et al., 2005). The current model can be regarded as an improvement on a previously published pre-vascularized skin model, which only enabled medium flow underneath the tissue and left out the perfusion of vessels in the construct (Helmedag et al., 2015). In this previous model the fluidic compartment was separated from the tissue by a porous membrane, limiting mass transport. In our approach the vasculature was experimentally accessible through the fluidic system of the bioreactor, and thereby the applicability domain is broader. This feature may improve prediction of transdermal skin absorption into the circulatory system.

5 Conclusion

Taken together, the vascularized skin equivalent represents an optimized organ model for scientific research. The vascularization for the first time enables the interaction of cellular and non-cellular-compartments of the blood stream with different layers of the tissue. This may be of particular interest with regard to immunological research and associated migration studies of lymphocytes. For clinical applications, the vascularized skin equivalent bears potential to be used as a vascularized skin graft for the treatment of deep skin wounds.

References

Braverman, I. M. (2000). The cutaneous microcirculation. *J Investig Dermatol Symp Proc 5*, 3-9. http://dx.doi.org/10.1046/j.1087-0024.2000.00010.x

De Wever, B., Petersohn, D. and Mewes, K. R. (2013). Overview of human three-dimensional (3D) skin models used for dermal toxicity assessment – part 1. *Household and Personal Care Today 8*, 18-23.

Fuchs, E. (2009). Finding one's niche in the skin. *Cell Stem Cell 4*, 499-502. http://dx.doi.org/10.1016/j.stem.2009.05.001

Gibot, L., Galbraith, T., Huot, J. et al. (2010). A preexisting microvascular network benefits in vivo revascularization of a microvascularized tissue-engineered skin substitute. *Tissue Eng Part A 16*, 3199-3206. http://dx.doi.org/10.1089/ten.TEA.2010.0189

Groeber, F., Holeiter, M., Hampel, M. et al. (2011). Skin tissue engineering – in vivo and in vitro applications. *Adv Drug Deliv Rev 63*, 352-366. http://dx.doi.org/10.1016/j.addr.2011.01.005

Groeber, F., Kahlig, A., Loff, S. et al. (2013). A bioreactor system for interfacial culture and physiological perfusion of vascularized tissue equivalents. *Biotechnol J 8*, 308-316. http://dx.doi.org/10.1002/biot.201200160

Groeber, F., Engelhardt, L., Egger, S. et al. (2015). Impedance spectroscopy for the non-destructive evaluation of in vitro epidermal models. *Pharm Res 32*, 1845-1854. http://dx.doi.org/10.1007/s11095-014-1580-3

Helmedag, M. J., Weinandy, S., Marquardt, Y. et al. (2015). The effects of constant flow bioreactor cultivation and keratinocyte seeding densities on prevascularized organotypic skin grafts based on a fibrin scaffold. *Tissue Eng Part A 21*, 343-352. http://dx.doi.org/10.1089/ten.TEA.2013.0640

Johnson, J. M., Brengelmann, G. L., Hales, J. R. et al. (1986). Regulation of the cutaneous circulation. *Fed Proc 45*, 2841-2850.

Knott, A., Koop, U., Mielke, H. et al. (2008). A novel treatment option for photoaged skin. *J Cosmet Dermatol 7*, 15-22. http://dx.doi.org/10.1111/j.1473-2165.2008.00356.x

Lei, X. H., Ning, L. N., Cao, Y. J. et al. (2011). NASA-approved rotary bioreactor enhances proliferation of human epidermal stem cells and supports formation of 3D epidermis-like structure. *PLoS One 6*, e26603. http://dx.doi.org/10.1371/journal.pone.0026603

Linke, K., Schanz, J., Hansmann, J. et al. (2007). Engineered liver-like tissue on a capillarized matrix for applied research. *Tissue Eng 13*, 2699-2707. http://dx.doi.org/10.1089/ten.2006.0388

Mertsching, H., Weimer, M., Kersen, S. et al. (2008). Human skin equivalent as an alternative to animal testing. *GMS Krankenhhyg Interdiszip 3*, Doc11.

Mertsching, H., Schanz, J., Steger, V. et al. (2009). Generation and transplantation of an autologous vascularized bioartificial human tissue. *Transplantation 88*, 203-210. http://dx.doi.org/10.1097/TP.0b013e3181ac15e1

Mildner, M., Jin, J., Eckhart, L. et al. (2010). Knockdown of filaggrin impairs diffusion barrier function and increases UV sensitivity in a human skin model. *J Invest Dermatol 130*, 2286-2294. http://dx.doi.org/10.1038/jid.2010.115

Montano, I., Schiestl, C., Schneider, J. et al. (2010). Formation of human capillaries in vitro: The engineering of prevascularized matrices. *Tissue Eng Part A 16*, 269-282. http://dx.doi.org/10.1089/ten.TEA.2008.0550

Novosel, E. C., Kleinhans, C. and Kluger, P. J. (2011). Vascularization is the key challenge in tissue engineering. *Adv Drug Deliv Rev 63*, 300-311. http://dx.doi.org/10.1016/j.addr.2011.03.004

Poschl, E., Schlotzer-Schrehardt, U., Brachvogel, B. et al. (2004). Collagen IV is essential for basement membrane stability but dispensable for initiation of its assembly during early development. *Development 131*, 1619-1628. http://dx.doi.org/10.1242/dev.01037

Pudlas, M., Koch, S., Bolwien, C. et al. (2011). Raman spectroscopy: A noninvasive analysis tool for the discrimination of human skin cells. *Tissue Eng Part C Methods 17*, 1027-1040. http://dx.doi.org/10.1089/ten.tec.2011.0082

Rossi, A., Appelt-Menzel, A., Kurdyn, S. et al. (2015). Generation of a three-dimensional full thickness skin equivalent and automated wounding. *J Vis Exp*. http://dx.doi.org/10.3791/52576

Schechner, J. S., Crane, S. K., Wang, F. et al. (2003). Engraftment of a vascularized human skin equivalent. *FASEB J 17*, 2250-2256. http://dx.doi.org/10.1096/fj.03-0257com

Scheller, K., Dally, I., Hartmann, N. et al. (2013). Upcyte(R) microvascular endothelial cells repopulate decellularized scaffold. *Tissue Eng Part C Methods 19*, 57-67. http://dx.doi.org/10.1089/ten.TEC.2011.0723

Shepherd, B. R., Enis, D. R., Wang, F. et al. (2006). Vascularization and engraftment of a human skin substitute using circulating progenitor cell-derived endothelial cells. *FASEB J 20*, 1739-1741. http://dx.doi.org/10.1096/fj.05-5682fje

Stark, H. J., Willhauck, M. J., Mirancea, N. et al. (2004). Authentic fibroblast matrix in dermal equivalents normalises epidermal histogenesis and dermoepidermal junction in organotypic co-culture. *Eur J Cell Biol 83*, 631-645. http://dx.doi.org/10.1078/0171-9335-00435

Supp, D. M., Wilson-Landy, K. and Boyce, S. T. (2002). Human dermal microvascular endothelial cells form vascular analogs in cultured skin substitutes after grafting to athymic mice. *FASEB J 16*, 797-804. http://dx.doi.org/10.1096/fj.01-0868com

Tremblay, P. L., Hudon, V., Berthod, F. et al. (2005). Inosculation of tissue-engineered capillaries with the host's vasculature in a reconstructed skin transplanted on mice. *Am J Transplant 5*, 1002-1010. http://dx.doi.org/10.1111/j.1600-6143.2005.00790.x

Walles, T., Giere, B., Hofmann, M. et al. (2004). Experimental generation of a tissue-engineered functional and vascularized trachea. *J Thorac Cardiovasc Surg 128*, 900-906. http://dx.doi.org/10.1016/j.jtcvs.2004.07.036

Yao, J., Maslov, K. I., Puckett, E. R. et al. (2012). Double-illumination photoacoustic microscopy. *Opt Lett 37*, 659-661. http://dx.doi.org/10.1364/OL.37.000659

Young, D. M., Greulich, K. M. and Weier, H. G. (1996). Species-specific in situ hybridization with fluorochrome-labeled DNA probes to study vascularization of human skin grafts on athymic mice. *J Burn Care Rehabil 17*, 305-310. http://dx.doi.org/10.1097/00004630-199607000-00005

Conflict of interest

The authors declare no conflict of interest.

Acknowledgements

The authors kindly thank the "Dr. Mildred Scheel Stiftung für Krebshilfe" (project title: 3-D Tumorprogression und Tumortherapie des Malignen Melanoms) and the Fraunhofer society for financial support of this work. Moreover, the authors are grateful for the partial support of J. Lange by the José Carreras Leukämie-Stiftung e.V. (DJCLS R 12/35).

Correspondence to

Dr Florian Groeber
Translational Center Würzburg, Fraunhofer Institute
for Interfacial Engineering and Biotechnology (IGB)
Röntgenring 11
97070 Würzburg
Germany
Phone: +49 172 7122331
e-mail: florian.groeber@igb.fraunhofer.de